Experimental study of blade thickness effects on the global and the local performances of axial-flow fans

Christophe Sarraf, Florent Ravelet, Hussain Nouri, Farid Bakir

HEFAT2010
7th International Conference on Heat Transfer, Fluid Mechanics and Thermodynamics
19-21 July 2010
Antalya, Turkey

EXPERIMENTAL STUDY OF BLADE THICKNESS EFFECTS ON THE GLOBAL AND THE LOCAL PERFORMANCES OF AXIAL-FLOW FANS

Sarraf C.*, Ravelet F., Nouri H. and Bakir F.
*Author for correspondence
Lab. Dynfluid, LEMFI,
Arts et Métiers - ParisTech,
151 Bd de l'Hôpital,
75013 Paris
France,
E-mail: christophe.sarraf@paris.ensam.fr

ABSTRACT

The study of Aerodynamic performance of axial-flow fans was carried out. Two fans that differ only in the thickness of their blades were studied. The first fan (F_{ref}), which is the reference, was designed to be part of the cooling system of an automotive vehicle power unit and has conventional thin blades. The second fan (F_{tck}) has much thicker blades compatible with the rotomoulding conception process that generates only hollow parts with large edge radius. The global performances of the fans were measured in a test bench designed according to the ISO-5801 standard. The curve of aerodynamics characteristics (pressure head versus flow rate) is slightly steeper for the fan with thick blades, and its efficiency is lower than the efficiency of the fan with thin blades.

To go further in the comparison, we also studied the wall pressure fluctuations at the casing wall in another normalized test bench, for two flow rates corresponding to the maximum efficiencies of the two fans. The total level of fluctuations is lower for the thick blades fan that for the thin blades fan, which is counter-intuitive. The spectral composition of the wall fluctuations are moreover very different for the two fans. These measurements will be used as a benchmark for high-order finite volume CFD codes developed for aeroacoustics in the laboratory.

INTRODUCTION

Until now, the axial fans used in the cooling system of automotive vehicles power unit are manufactured by plastic injection, a process widely used in large series production. Some fans of large size, set in truck power units or in large air cooler systems, are produced in small quantities and the plastic injection is not cost-effective in that case. The rotomoulding process, previously tested for wind turbine blades [1], can provide an economic answer if it is shown that the performances of the fans obtained by this process are of sufficient quality.

In aeronautics and in the automotive industry, changing the blade thickness has been used for many years as an efficient way to modify the lift and drag characteristics [2], [3], and the boundary layers detachment process [4]. Applied to low-speed axial fans, the extra thickness increases the power of the elementary noise sources so that the noise generated by von Kármán street is higher for thick blades fans than for thin blades ones. A complete literature on aerodynamic and acoustic properties of axial fans with swept blades is presented in [5].

The aim of this paper is to determine the thickness effects on the global performance of axial fans and the pressure fluctuations which occur in their wake.

NOMENCLATURE

qv	[m^3/s]	flow rate
c	[m]	chord length
x/c	[-]	relative chord wise location
C	[Nm]	torque
f	[Hz]	frequency
F	[-]	fan
D	[mm]	ducting pipe diameter

Special characters

η	[-]	static efficiency
ω	[rad/s]	rotation speed
Φ	[-]	flow coefficient
Ψ	[-]	pressure coefficient
Δp	[Pa]	static pressure

Subscripts

N	Nominal
eff	effective
ref	reference fan (thin blades)
tck	thick blades fan
ext	External
int	Internal
bpf	Blade Passing Frequency
Max	Maximum
0	Ambient or reference

EXPERIMENTAL SETUP

1- Geometry of the two tested axial-flow fans

The fans used in this study are two prototypes developed for automotive engine cooling system applications following the methods detailed in [6], [7], [8]. The fans have the same geometrical characteristics except the blade thickness. Pictures of the thick blades fan are displayed in Figure 1 with a schema of a span-wise section of thick and thin blades.

Each of these fans has six blades. The hub-to-tip radius ratio is $R_{int}/R_{Max} = 0.366$ with the tip radius $R_{Max} = 179$ mm. The rotor is built up from blades of circular-arc camber lines, with NACA 4-digits-based profiles clipped at 0.95 x/c. The maximum blade thickness of the thin blade axial-flow fan (F_{ref}) is 4mm. The second fan (F_{tck}), had blades homothetically thickened to reach a maximum thickness of 10 mm. The blades are swept forward in order to increase the efficiency of the fan. Fukano *et al.* [9] have shown that fans with forward swept blades are superior to those with backward swept blades in terms of global and acoustical performances. The Fan F_{ref} was designed to meet the specifications point $\Delta p = 270$ Pa, $qv_N = 2650$ m^3/h for a nominal rotation speed $\omega_N = 260$ rad/s.

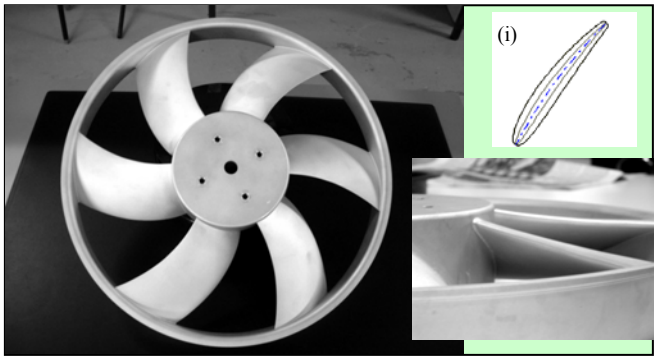

Figure 1: Views of the thick blades fan. (i) Section of thick and thin profiles.

2- Free-flow experimental facility

The Figure 2 shows the experimental facility used to determine the global performances of the fans. The air suction test bench was designed and built at the Dynfluid-LEMFI laboratory of Arts et Métiers ParisTech according to the ISO 5801 standard [10]. The air flow rate is set and measured according to the ISO-5167 norm [11] by setting the hydraulic impedance of the bench through diaphragms of various sizes.

Figure 2: ISO 5801 air test bench, Dynfluid-LEMFI / Arts et Métiers ParisTech. The dimensions are 1.3 x 1.3 x 1.8 m.

Elevation pressures Δp are measured with an absolute precision of ± 0.1 Pa. The torque on the fan shaft is measured with a HBM strain gauge transducer. The uncertainty of torque measurements corresponds to 0.1% of the maximum measured torque. The angular velocity ω is measured with a tachymeter of relative precision ± 0.2%. The power absorbed on the fan shaft is then estimated through the product $C\,\omega$. The accuracy of the whole system leads to a determination of the efficiency within about ± 0.5%.

3- Ducted-flow experimental facility

In order to compare the behaviour of the two fans in a ducted-flow configuration, a second test bench was built according to the ISO-5801 norm (Figure 3). It consists of a cylindrical pipe of inner diameter D = 380mm.

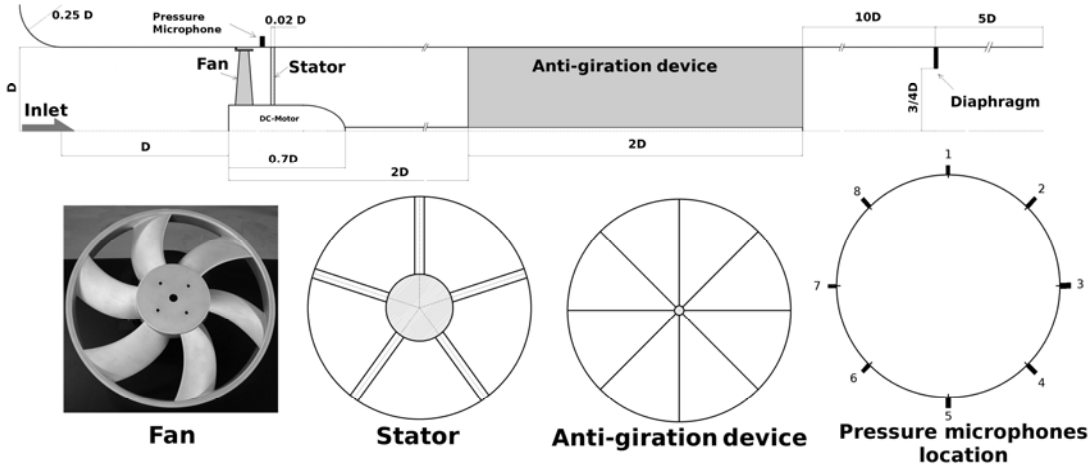

Figure 3: Ducted-flow configuration dedicated to global and local measurements.

A bell mouth is flush-mounted at the inlet of the duct. The upstream face of the fan is at a distance D from the pipe inlet. A DC-motor is hidden in a casing of diameter 0.3 D and length 0.7 D, with a warhead-shape end. The binding to the tube is ensured by five rods of diameter 8mm, i.e. 0.02 D, in order to minimize their influence, regardless the flow rate. The distance between the upstream face of the fan and the binding rods is 0.26 D. An anti-gyration device made of eight metal sheets of thickness 1.5mm and length 2 D is placed 2 D downstream of the rotor-stator set. It prevents the outgoing flow from having any rotating component. The static pressure of the axial fan is measured 1 D downstream of the anti-gyration device, with an average over four flush-mounted pressure taps. The flow rate is measured with a normalized diaphragm, located 10 D downstream of the anti-gyration device and 5 D upstream of the pipe outlet. The diaphragm has a diameter of 0.73 D. Other diaphragms of various sizes are placed at the exit of the pipe to vary the test-bench hydraulic impedance and thereby to vary the operating point of the studied axial-flow fan. Wall pressure fluctuations are measured simultaneously by eight microphones that are evenly distributed on the circumference of the duct. They are mounted downstream of the fan, halfway between the fan and the five rods that ensure the binding to the tube (see Figure 3). The microphones are G.R.A.S 40BP 1/4" polarized pressure microphones of sensitivity 1.65 mv.Pa^{-1}, with G.R.A.S 26AC preamplifiers and a G.R.A.S 12AG power supply module. The signals are amplified with a gain of +30 dB and high-pass filtered with a three-pole Butterworth filter with cut-off frequency of 20 Hz. The signals are then digitalized using a NI Data Acquisition Card (M 6211, 16 bits) at a sample rate of 12 kHz.

FANS GLOBAL CHARACTERISTICS

The characteristics of the two fans are shown in Figure 4 together with the designed specifications point of the reference fan. Flow coefficient (Φ) and pressure coefficient (Ψ) are defined respectively by equations (1) and (2):

$$\phi = \frac{qv}{\pi\omega R_{Max}^3} \qquad (1),$$

$$\psi = \frac{\Delta p}{\rho\omega^2 R_{Max}^2 / 2} \qquad (2),$$

The design point thus corresponds to $\Phi = 0.156$ and $\Psi = 0.200$.

The curves are the results of five measurements proceeded at nominal rotation speed ω_N. The error bars in Figure 3 stand for the RMS (root mean square) values of the five measurements of Φ and Ψ, magnified by a factor three for better visualization. The pressure coefficient distributions are globally relatively similar to each other. The thin blades fan (F_{ref}), matches the specifications point plotted in Figure 4. At the design flow rate, the thick blades fan (F_{tck}) produces a depression 8% below the specified depression. As shown in the figure, the curve of F_{tck} is steeper than the one of F_{ref}. At partial flow rates below $\Phi = 0.11$, F_{tck} produces more depression than F_{ref}. At overflow rates, approximately beyond $\Phi = 0.2$, the difference of depression between the two fans remains almost constant.

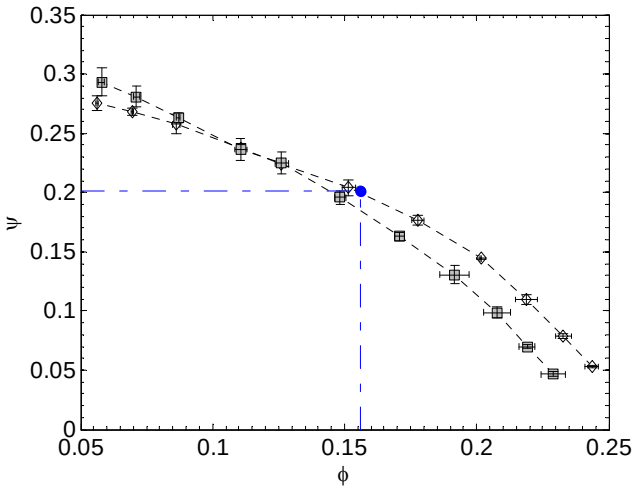

Figure 4: Fans characteristics: Pressure coefficient Ψ *vs.* flow coefficient Φ. ■ thick blades fan, ◊ thin blades fan. + reproducibility evaluated from 5 independent experiments (x3). ● Design specification point.

The relative position of the two curves is consistent with the specificity of thick aerodynamic profiles [12]: partial flow rates imply high angle of incidence between the profile and the flow directions. Firstly, in the case of thick profiles, the boundary layer separation on the upper surface can be less important for the same angle of incidence and the fan remains more able to produce depression as it seems to occur in this experiment. Secondly, at nominal flow rate and overflow rates, thick profiles are known to produce more viscous dissipation, especially when they have rounded trailing edge as it is the case here. Thirdly, these profiles can also be subject to lower surface separations [13]. These points can explain the lack of depression produced by F_{tck} at overflow rates. At partial flow rates, it should be noticed that the flow downstream of the fan has a very important radial component, not already quantified but classically observed by Kergoulay *et al.* [14]. Furthermore we have observed that the pressure elevations and the torques are significantly fluctuating at these partial flow rate operating points.

The efficiencies of both fans are shown in figure 5 with the specifications flow rate coefficient of the fan F_{ref}. Efficiency coefficient (η) is defined by equation (3):

$$\eta = \frac{C\omega}{\Delta p q_v} \qquad (3),$$

The efficiencies distributions have a classical shape, skewed toward partial flow rates, with a strong fall after the nominal flow rate which is fairly set around an overflow of about 20%. At $\Phi = 0.18$ and $\Psi = 0.17$, F_{ref} reaches its maximum efficiency of $\eta_{Max\ ref} = 0.58 \pm 0.005$ which is pretty fair for this type of turbomachinery [6]. The maximum of η is shifted toward overflow with respect to the design point. One open question is whether this is due to the forward swept or not.

The maximum efficiency of F_{tck} reaches a value $\eta_{Max\ tck} = 0.55 \pm 0.005$. The thickening of the blades has led to a decrease of 0.03 of η. The maximum of η is shifted toward a partial flow of about 30% with respect to the nominal flow rate of F_{ref} and the thick blades fan thus gives its best efficiency for a flow rate $\Phi = 0.15$ very close to the design point. The corresponding pressure coefficient is $\Psi = 0.19$.

The distribution of the efficiency of F_{tck} is moreover flatter than that of F_{ref}: quantitatively, the range of flow rates corresponding to a decrease of 3% of η from η_{Max} is $\pm 0.3\ \Phi/\Phi_N$ for F_{tck}, while it is only $\pm 0.2\ \Phi/\Phi_N$ for F_{ref}.

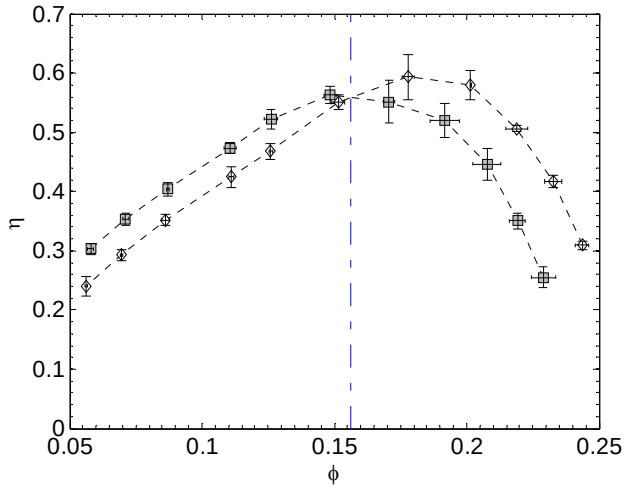

Figure 5: Fan efficiency η *vs.* flow coefficient Φ. ■ thick blades fan, ◊ thin blades fan. + reproducibility evaluated from 5 independent experiments (x6). The vertical dash-dotted line corresponds to the design point flow coefficient.

As a partial conclusion please also note that although the thick blades fan F_{tck} does not meet the specification point at the nominal angular velocity $\omega_N = 260$ rad/s, the desired point in a dimensional point of view ($\Delta p = 270$ Pa, $qv_N = 2650$ m^3/h) can be reached with this fan rotating at $\omega = 270$ rad/s. Since the efficiency of the two fans is the same at such flow rates (η=0.55), the use of F_{tck} at $\omega = 270$ rad/s in the automotive cooling application would lead to the very same power consumption as the use of F_{ref} at $\omega_N = 260$ rad/s.

In the next section, we further investigate the consequences of a use of the thick blades fan in terms of pressure fluctuations that are an image of the acoustical performances by measurements in the ducted-flow test facility.

PRESSURE FLUCTUATIONS

The results of this paragraph concern the two axial-fans operating in a ducted-flow configuration (Figure 3). In that case there is a radial gap of 1.5 mm between the pipe and the collar surrounding the fan. It should be also noted that for technical reasons, the ducted experiments have been performed for an angular velocity of 209.5 rad/s (2000 rpm). The presence of the gap substantially reduces the global efficiency of the fans without modifying perceptively the nominal flow rate: the F_{ref} fan reaches a maximum efficiency $\eta_{Max\ ref} = 0.49$ for a flow coefficient $\Phi = 0.18$. The pressure coefficient is $\Psi = 0.15$, slightly lower than in the free-flow experiment which presents no radial gap. The F_{tck} fan reaches a maximum efficiency $\eta_{Max\ tck} = 0.48$ at a flow coefficient $\Phi = 0.15$ and a pressure coefficient $\Psi = 0.18$. The characteristic curves show similar behaviour as in the free-flow case.

The wall pressure fluctuations are compared for two different flow rates, corresponding to the nominal point of the thin blades fan $\Phi_{ref} = 0.18$ and the nominal point of the thick blades fan $\Phi_{tck} = 0.15$. In every case, for a fixed diaphragm at the pipe exit, the angular velocity of one of the two fans has been set to $\omega = 209.5$ rad/s and the angular velocity of the second fan has been adjusted in order to give the same dimensional pressure elevation and flow rate for the two fans.

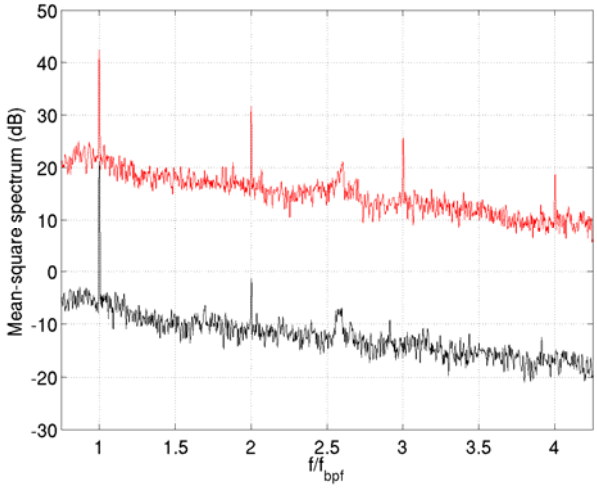

Figure 6: Square amplitude spectra of wall pressure fluctuations for thin blades axial-flow fan F_{ref} (black) and thick blades axial-flow fan F_{tck} (red) at a flow rate $\Phi = \Phi_{ref}$=0.18. F_{ref} rotates at $\omega = 209.5$ rad/s and F_{tck} rotates at $\omega = 211.5$ rad/s. The F_{tck} spectrum has been shifted by +30 dB for clarity.

The squared amplitude spectra of wall pressure at Φ_{ref} are plotted in Figure 6. The spectra *S(f)* are expressed in dB using the formula

$$S(f) = 20\log_{10}\left(|p'(f)|/p_0\right)$$

with *p'(f)* the modified Welch-average Fourier Transform of the fluctuating pressure. The sampling time is 10s, corresponding to approximately 330 fan rotations, and the spectra is an average of eight 50% overlapping parts, windowed with a Hamming window. The spectra are displayed between 150 and 850 Hz.

Both fans exhibit relatively high discrete peaks, corresponding to the blade passing frequency f_{bpf} (200 Hz for F_{ref} and 202 Hz for F_{tck}) and its harmonics. They are high above the broadband noise. The two fans differ however strongly by the repartition of energy between the different harmonics. For the F_{ref} fan, only the fundamental frequency f_{bpf} and the first harmonic $2f_{bpf}$ are visible. The level at f_{bpf} is 21 dB, and the level at $2f_{bpf}$ is 1.5 dB. For the F_{tck} fan, the first three harmonics clearly appear. At the blade passing frequency f_{bpf} the level is 12 dB. At $2f_{bpf}$ it is 2 dB, at $3f_{bpf}$ it is -4 dB and at $4f_{bpf}$ it is -11 dB. For this flow rate, the increase of blades thickness thus seems to lead to a decrease of the first peak level, and to an increase of the harmonics. The global level of fluctuations, *i.e.*

$10\log_{10}(\sigma_{p'}^2 / p_0^2)$, is moreover lower for the thick blades fan (19 dB) than for the thin blades fan (23 dB).

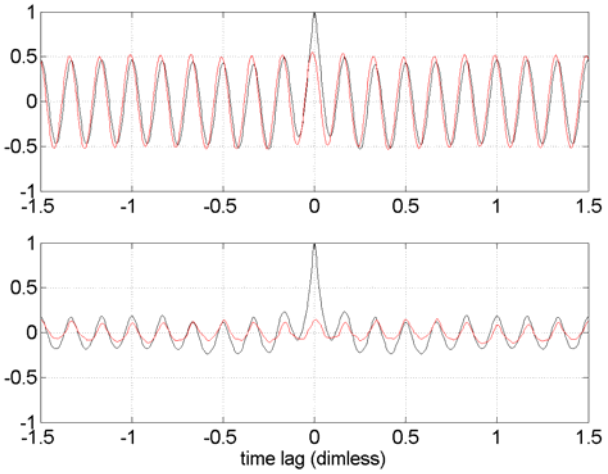

Figure 7: Black curves: autocorrelation function of pressure fluctuations at position 1 (see Figure 3). Red curves: cross-correlation function of pressure fluctuations between position 1 and position 5 (see Figure 3). Top graph corresponds to the F_{ref} fan at Φ_{ref}=0.18, bottom graph corresponds to the F_{tck} fan at Φ_{ref}=0.18. The time is made non-dimensional with reference to one period of rotation: $\tau = t \times \frac{\omega}{2\pi}$

Figure 7 presents autocorrelation and cross-correlation functions of wall pressure fluctuations for the two fans. The black curves correspond to the autocorrelation function:

$$A(\tau) = \frac{\langle p_1'(t).p_1'(t-\tau)\rangle}{\sigma_{p_1'}^2};$$

and the red curves correspond to the cross-correlation function between microphones 1 and 5:

$$C_{1-5}(\tau) = \frac{\langle p_1'(t).p_5'(t-\tau)\rangle}{\sigma_{p_1'}.\sigma_{p_5'}}.$$

One can notice that the functions present a periodicity that corresponds to six events in one rotation that is the blade passing frequency. The time lag for the strongest peak in the cross-correlation function does match the angular distance between the microphones which is one half of a turn here. Another common feature between the two fans is that secondary peaks height for the autocorrelation function are close to the peaks height for the cross-correlation function. Some strongly coherent flow structures might be involved in this zone between the rotor and the binding static part. The strong difference between the F_{ref} fan and the F_{tck} fan is the value of the cross-correlation coefficient. It is significantly lower for the thick blades fan. Local velocity measurements that give access to flow structure such as PIV measurements would be of great interest in order to better understand this difference.

The previously described features regarding both the spectral composition and the relative fluctuations levels could be due to the fact that the F_{ref} fan is working at its nominal flow rate while the F_{tck} fan is working at overflow rate. To answer this question we have performed the following experiment.

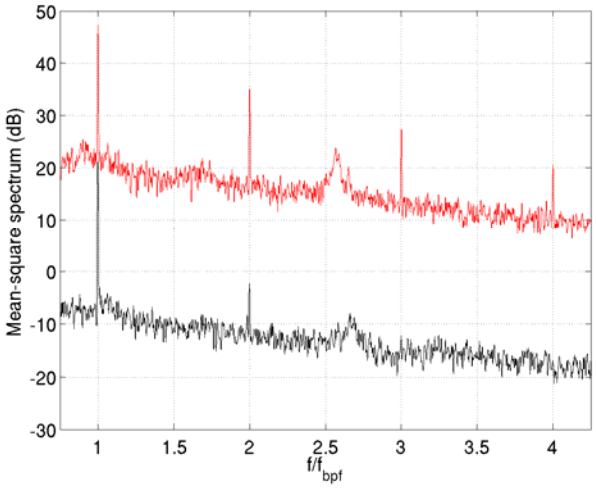

Figure 8: Square amplitude spectra of wall pressure fluctuations for thin blades axial-flow fan F_{ref} (black) and thick blades axial-flow fan F_{tck} (red) at a flow rate $\Phi = \Phi_{tck} = 0.15$. F_{tck} rotates at $\omega = 209.5$ rad/s and F_{ref} rotates at $\omega = 202.7$ rad/s. The F_{tck} spectrum has been shifted by +30 dB for clarity.

The squared amplitude spectra of wall pressure at the nominal flow rate of the thick blades fan $\Phi_{tck} = 0.15$ are plotted in Figure 8. The blade passing frequency is now $f_{bpf} = 200$ Hz for F_{tck} and 193 Hz for F_{ref}. Please not that the angular velocity ratio needed to reach the same dimensional static pressure elevation and flow rate $\omega_{tck} / \omega_{ref} = 1.037$ is the same as the ratio discussed in the last paragraph of the section dedicated to the fan global characteristics.

The results are very similar to the previously described flow rate: for the F_{ref} fan, the fundamental frequency f_{bpf} and the first harmonic $2f_{bpf}$ are still the only visible peaks in the spectrum. The level at f_{bpf} is 21 dB, and the level at $2f_{bpf}$ is -2 dB. For the F_{tck} fan, the first three harmonics clearly appear. At the blade passing frequency f_{bpf} the level is 17 dB. At $2f_{bpf}$ it is 5 dB, at $3f_{bpf}$ it is -2.5 dB and at $4f_{bpf}$ it is -9.5 dB. The decrease of the first peak level and the increase of the level of the harmonics is also present at this flow rate. The global level of fluctuations is 20 dB for the thick blades fan and 22.5 dB for the thin blades fan.

CONCLUSION

Two fans that differ only in the thickness of their blades were studied in order to highlight the effects of thickness on global performances and pressure fluctuations generated. The first fan, which has conventional thin blades, was designed to be part of the cooling system of an automotive vehicle power unit. The second compatible with the rotomoulding conception process, that generates only hollow parts with large edge radius, has much thicker blades. The performances of the fans were measured and the results indicate that the global performances were substantially equivalent, with a drop of 8% of pressure elevation at conception flow rate for the thick blades fan and a

maximum efficiency that is 3% lower than the efficiency of the thin blades fan and that is shifted towards lower flow rates. Contrary to what one could *a priori* think the thick blades fan does present a certain number of interesting features. Its efficiency curve is clearly flatter and the conception point can be reached by a relative increase of rotational speed of 4% for the same power consumption. In terms of the automotive cooling system application, the fact that the characteristic curve is steeper is positive: the flow rate is more stable with respect to small variations of the circuit hydraulic impedance. The wall pressure fluctuations just downstream of the fan are moreover lower for the thick blades. Finally, at very partial flow rates, the thick blades fan produces more elevation than the thin blades fan, which could be beneficial concerning pumping instabilities.

Further investigations are needed to better understand the effects of the blades thickness. The local pressure fluctuations measurements will be performed at other positions and for partial flow rates together with LDV and PIV measurements and numerical simulations in order to highlight flow separation process, unsteadiness around fan blades and wake interactions . These measurements will be used as a benchmark for high-order finite volume CFD codes developed for aeroacoustics in the laboratory, and data are also available on request.

REFERENCES

[1] Tcharkhtchi A., Rotomoulage de pièces en matière thermoplastique (Rotomolding of thermoplastic parts). (2004), Techniques de l'ingénieur. Plastiques et composites ISSN 1762-8776. vol. AM4, noAM3706, pp. AM3706.1-AM3715 (31 ref.).

[2] Thwaites B., Incompressible Aerodynamics, An Account of the Theory and Observation of the Steady Flow of incompressible Fluid past Aerofoils, Wings, and Other Bobies. (1987) Dover Publication, Inc.

[3] Hoerner S. F., “Fluid-Dynamic Lift”. (1985) edition Hoerner Fluid Dynamics.

[4] C.Sarraf, H. Djeridi, J.Y. Billard, (2008). “ Effets d'épaisseur et couche limite sur profil portant. Effets de l'épaisseur des profils NACA symétriques sur leurs performances et l'état de la couche limite turbulente ”, European Journal of Environmental and Civil Engineering, VOL 12/5 - 2008 - pp.587-599.

[5] Wright T, Simmons WE. Blade sweep for low-speed axial fans. Journal of Turbomachinery 1990;(January):151–8.

[6] Noguera, R., Rey, R., Massouh, F., Bakir, F., and Kouidri, S., 1993, “Design and Analysis of Axial Pumps,” ASME Fluids Engineering, Second Pumping Machinery Symposium, pp. 95–111, Washington, USA.

[7] Bakir, F., Rey, R., and Moreau, S., “Latest Developments in Automotive Engine Cooling Fan Systems Rotor-Stator Interactions,” FEDSM99-7331, SanFrancis co, July 1999.

[8] Bakir F., Moreau S., Rey R., Henner M., Borg V. "Experimental aeroacoustic analysis of efficient automotive engine cooling fan systems" (2003) Fan Noise 2nd Int. Symp., pp. 18, 19 – Senlis 2003.

[9] Fukano, T., Kodama, Y., Takamatsu, Y. Noise generated by low pressure axial flow fans, III: Effects of rotational frequency, blade thickness and outer blade profile (1978) Journal of Sound and Vibration, 56 (2), pp. 261-277.

[10] ISO 5801 - Industrial fans Performance testing using standardized airways, 2007, International Standards for Business, Government and Society,

[11] ISO 5167 - Measurement of fluid flow by means of pressure differential devices inserted in circular cross-section conduits running full, 2003, International Standards for Business, Government and Society,

[12] Sarraf C., Jaouen R., Djeridi H., “Investigation of thickness effects on 2D NACA symmetric foils”. (2005). Proceedings Ocean05.

[13] J. Estevadeordal, S. Gorgineni, W. Copenhaver, G. Bloch, M. Brendel, Flow field in a low-speed axial fan: a DPIV investigation, Exp. Thermal Fluid Sci. 23 (2000) 11–21.

[14] Kergourlay G., Kouidri S., Rankin G.W. and Rey R., Experimental investigation of the 3D unsteady flow field downstream of axial fans, Flow Measurement and Instrumentation, Vol. 17, 2006, pp. 303-314.